Results in Physics 19 (2020) 103411

Contents lists available at ScienceDirect

Results in Physics

journal homepage: www.elsevier.com/locate/rinp

Near-infrared quantum cutting in Tm^{3+}/Yb^{3+}-doped phosphate glasses

Dong-Yang Shi [a], She-bao Lin [a,b,*], Xiao-xia Zhao [c], Ai-ling Feng [a], Qiang Xu [a]

[a] Institute of Physics & Optoelectronics Technology, Baoji University of Arts and Sciences, Baoji 721016, China
[b] Advanced Titanium Alloys and Functional Coatings Cooperative Innovation Center, Baoji 721016, China
[c] School of Physics and Electronic Information Engineering, Henan Polytechnic University, Jiaozuo 454003, China

ARTICLE INFO

Keywords:
Phosphate glasses
Tm^{3+}/Yb^{3+}
Quantum cutting

ABSTRACT

A series of phosphate glasses with compositions of $30SrO\text{-}60P_2O_5\text{-}10Na_2O\text{-}0.5Tm_2O_3\text{-}xYb_2O_3$(x = 0, 1, 5, 9, 11 in mol%) were manufactured by melt-casting method, the quantum cutting between the Tm^{3+} and Yb^{3+} in the phosphate glasses is investigated, the energy transfer from Tm^{3+}:$^1G_4$ to Yb^{3+}:$^2F_{5/2}$ is proved. According to calculate, the highest quantum efficiency is up to 159.9%, the emission wavelength is at 1020 nm, matching the energy band gap of a silicon solar cell well, therefor, these phosphate glasses could potentially be used in silicon solar cells.

Introduction

The worldwide energy crisis has drawn the attention of scientists from all over the world [1]. In recent years, a constant effort has been made by researchers to utilize solar energy for the solar energy is no pollution and rich reserves [2,3]. An important method of using solar energy is photoelectric conversion. Silicon-based solar cells are essential devices for photoelectric conversion. The energy of the solar spectrum is concentrated in the short wavelength range, while the energy band gap of crystalline silicon is 1.12ev that lies in the infrared band [4,5], therefore, the sunlight spectra is not match the band gap of the silicon solar cell. As a result, the most soar energy can not be obsorbed by the solar cell and the heating effect is severe. However, this problem can be effectively solved by using quantum cutting (QC), QC refers to the energy transfer process that the rare-earth ion emits two protons after rare-earth ion absorption one high-energy ultraviolet photon [3,6]. The quantum cutting was put forward by Dexter in 1957 firstly [7,8], since then, scientists have carried out extensive research on quantum cutting. So far, the quantum cutting is used in the fields of plasma display, mercury-free fluorescent tubes, solar cells and so on [8]. The rare earth ion pairs commonly used in the study of quantum cutting are Tm^{3+}/Yb^{3+}, Tb^{3+}/Yb^{3+}, Ce^{3+}/Yb^{3+}, Eu^{2+}/Yb^{3+}, Pr^{3+}/Yb^{3+}, Nd^{3+}/Yb^{3+} and so on [8–11].

Tm^{3+}/Yb^{3+} doped glasses have been researched widely since these glasses play the important role as the optical systems converting near-infrared radiation into visible (blue) light or emitting near-infrared radiation at about 1800 nm, and the effects of Tm^{3+}/Yb^{3+} energy transfer and back transfer are also observed [12–17]. Especially, this ion pairs can also convert the blue light into near-infrared light which overcomes the problem of low energy conversion efficiency of solar cells. In this pair of ions, the wavelength of the transition of Yb^{3+}:$^2F_{5/2}\rightarrow{}^2F_{7/2}$ is about 1000 nm which equal to the band gap of crystalline Si and Tm^{3+} ion possesses the energy level that is around double times of Yb^{3+} [18]. Through QC, the Tm^{3+} transfer the energy to the Yb^{3+}, thus Tm^{3+} acts as an absorber to absorb the blue light which is difficult to be absorbed by silicon solar cells and the Yb^{3+} acts as an emitter to emit near-infrared light that can be absorbed by silicon solar cells, the solar cell efficiency can be greatly improved, the maximum quantum efficiency can reach 200%[19].

In this paper, Tm^{3+}/Yb^{3+} doped phosphate glasses were prepared. Based on XRD pattern, the absorption spectra, the excitation spectra, emission spectra and decay curve, the nature of the samples, energy level structure, energy transfer process and quantum efficiency between the Yb^{3+} and Tm^{3+} are discussed, the results show these phosphate glass system possesses great potential application in silicon solar cells.

Experimental

A group of phosphate glasses with chemical formula of $30SrO\text{-}60P_2O_5\text{-}10Na_2O\text{-}0.5Tm_2O_3\text{-}xYb_2O_3$(x = 0, 1, 5, 9, 11 in mol%, labeled as TY0, TY1, TY5, TY9, TY11) were prepared by high temperature melting method. SrO and Na_2O are introduced by $SrCO_3$ and Na_2CO_3 respectively, P_2O_5 is introduced by $NH_4H_2PO_4$. High-purity chemical raw materials were weighed 15 g in proportion and mixed evenly, then

* Corresponding author.
E-mail address: linshebao@163.com (S.-b. Lin).

https://doi.org/10.1016/j.rinp.2020.103411
Received 28 May 2020; Received in revised form 8 September 2020; Accepted 13 September 2020
Available online 17 September 2020

melted in a 1200℃ muffle furnace for 1 h. After that, the molten glass liquid was poured on a preheated copper plate, and annealed at 450℃ for 6 h, then cooled to room temperature. All specimens were buffed to a thickness of 5 mm for subsequent test.

The X-Ray diffraction (XRD) pattern for samples was examined by X-ray diffractometer (Bruker D2 PHASER, Germany) with a Cu Kα source and in a step of 0.02°. The absorption spectrum was measured by a UV/VIS/NIR spectrophotometer (JASCO V-770, Japan) with a resolution of 0.5 nm, the excitation spectra, emission spectra and decay curve were tested by a fluorescence spectrophotometer (Edinburgh Instrument. FLS980, UK) with a resolution of 1 nm and 1us.

Results and discussion

XRD pattern for samples

Fig. 1.is the XRD pattern of TY glass samples. As shown, all the XRD patterns of TY glasses are similar and there are no sharp crystalline peaks in the XRD patterns. These indicate the phases in the samples are amorphous and there are no crystals in the samples.

Absorption spectra for samples

Fig. 2.is the the absorption spectra of TY glass samples, there are six absorption peaks at 357, 467, 685, 791, 976 and 1212 nm respectively. One strong peak at 976 nm belongs to the transition of Yb^{3+}:$^2F_{7/2}\rightarrow{}^2F_{5/2}$, other five peaks at 357, 467, 685, 791 and 1212 nm are attributable to the transitions of Tm^{3+}: $^3H_6\rightarrow{}^1D_2$, $^1G_4$, $^3F_{2,3}$, $^3H_4$ and $^3H_5$, respectively [20]. Since TY0 is not doped with Yb^{3+}, there is no peak at 976 nm in TY0 glasses. The wavelength of the absorption ultraviolet cut-off edge of TY sample increase with the content of Yb^{3+}, this red shift phenomenon of absorption cutoff edge could be caused by the polarization of Yb_2O_3. Meanwhile, compared the absorption intensity of TY glasses in 976 nm, as the the Yb^{3+} conscentration increases, the absorption spectra intensity of samples increases obviously, this is because with Yb^{3+} concentration increasement, Yb^{3+} ions absorb more photons, which leads to the enhancement of material absorption.

Quantum cutting luminescence

Figs. 3and 4show the visible and near infrared emission spectra of TY samples excited by 467 nm light, with increase the content of Yb_2O_3, the intensity of the sharp peak at 650 nm (assigned to Tm^{3+}:$^1G_4\rightarrow{}^3F_4$ transition [3]) of the samples decreases, meanwhile, the intensity of the peak at 1020 nm of samples from TY1 to TY9 increases, but TY11

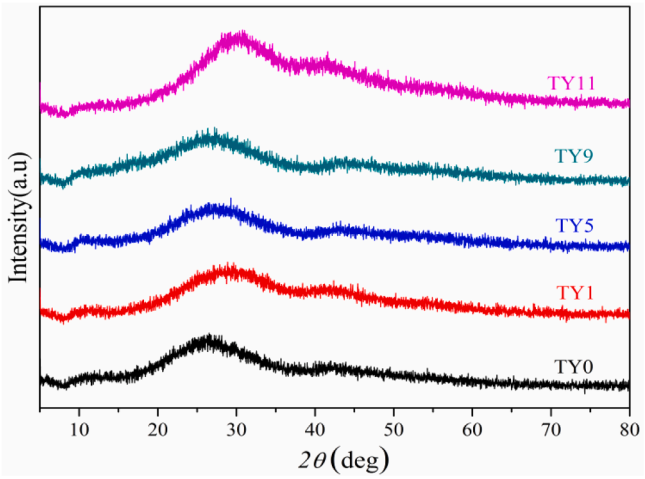

Fig. 1. XRD pattern of TY glass samples.

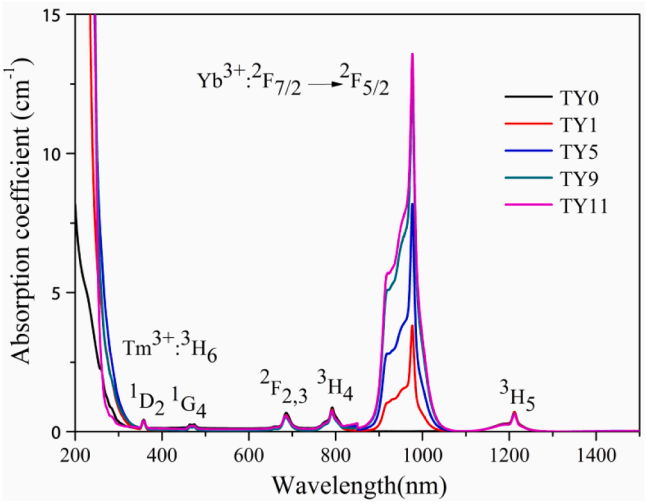

Fig. 2. The absorption spectra of TY glass samples.

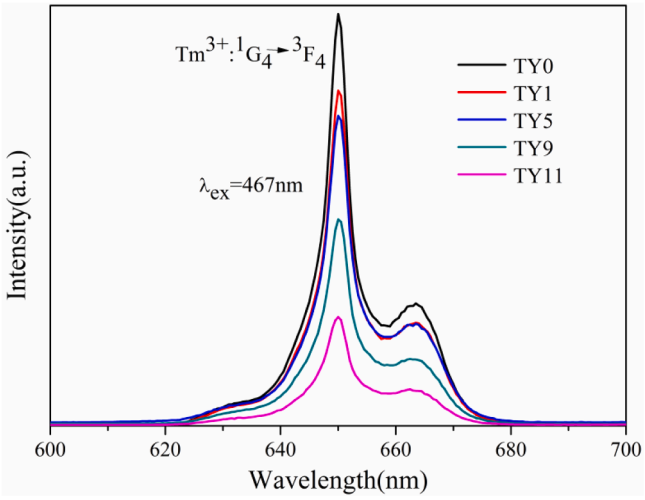

Fig. 3. The emission spectra in visible region of TY samples excited by 467 nm light.

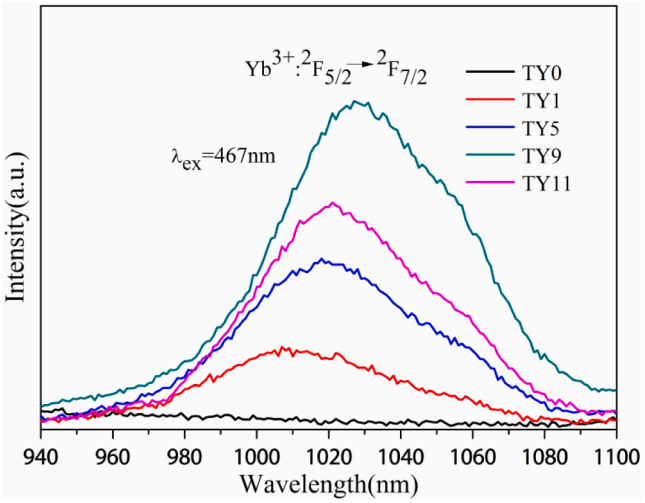

Fig. 4. The emission spectra in near infrared region of TY samples excited by 467 nm light.

decreases. This phenomenon can be explained by the quantum cutting theory; Tm^{3+} ions transfer their energy to Yb^{3+} ions which emit two photons with the wavelength of 1020 nm. The specific process is shown in Fig. 5, as the samples are excited by 467 nm light, Tm^{3+} absorbed one photon and jumps from $^3H_6$ ground state to $^1G_4$ excited state, due to the energy of photon at 467 nm is over twice the photon at 1020 nm, the Tm^{3+} transfers its energy to two Yb^{3+} ions, Yb^{3+} emits two near-infrared photons at 1020 nm and go back to ground state. However, as the Yb^{3+} concentration goes up to 11 mol%, concentration quenching leads to the decrease of emission intensity at 1020 nm.

Fig. 6 is the excitation spectra of TY9 sample monitoring at 650 nm and 1020 nm. As Fig. 6 shows, a sharp and broader peak excitation appeared in 450–490 nm range that was attributed to Tm^{3+}:$^3H_6 \rightarrow {}^1G_4$ transition. As is known to all, single doped Yb^{3+} cannot generate emission spectra at 1020 nm under 467 nm excitation. But in Fig. 6, monitoring at 650 nm and 1020 nm, the excitation spectra of TY9 sample are almost same except for the intensities, this shows that there is only one possibility, that is, Tm^{3+} absorbs photons and transmits energy to Yb^{3+} ions, and Yb^{3+} emits 1020 nm light, this also illustrates existing the quantum cutting between Tm^{3+} and Yb^{3+} ions.

Decay curves

Fig. 7 gives the decay curves of Tm^{3+}:$^1G_4 \rightarrow {}^3F_4$ of TY samples excited by 467 nm light. the decay curves match the double exponential function very well, the functional expression is as following[22–24]:

$$I(t) = A_1 exp(-t/\tau_1) + A_2 exp(-t/\tau_2) + B \quad (1)$$

Here $I(t)$ is the luminescence intensities; A_1, A_2 and B are the constants; τ_1 and τ_2 are the lifetimes for the exponential components, respectively. The decay lifetime of the glass can be caculated by [22,24]:

$$\tau = \frac{A_1\tau_1^2 + A_2\tau_2^2}{A_1\tau_1 + A_2\tau_2} \quad (2)$$

The concrete values and the changing trend of decay time at 650 nm are shown in Figs. 7 and 8. The results show the decay time decreases from 105 us to 42 us with increasement of Yb^{3+} concentration. The reasons are as follows: when Tm^{3+} is excited to excited state $^1G_4$ by 467 nm excitation, Tm^{3+} ion release energy in two ways: one is that Tm^{3+} directly transition from $^1G_4$ to $^3F_4$ and emits the 650 nm light, the other is that Tm^{3+} transfers energy to two Yb^{3+} ions through cooperative transfer, which makes Yb^{3+} emits two near-infrared (~1020 nm) photons. As the Yb^{3+} concentration increases, the energy that transfers from

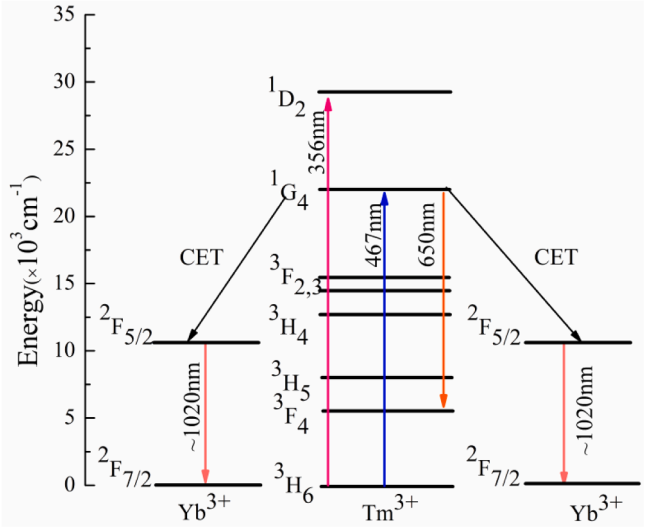

Fig. 5. The quantum cutting mechanism in Tm^{3+} and Yb^{3+} in TY samples [18,21].

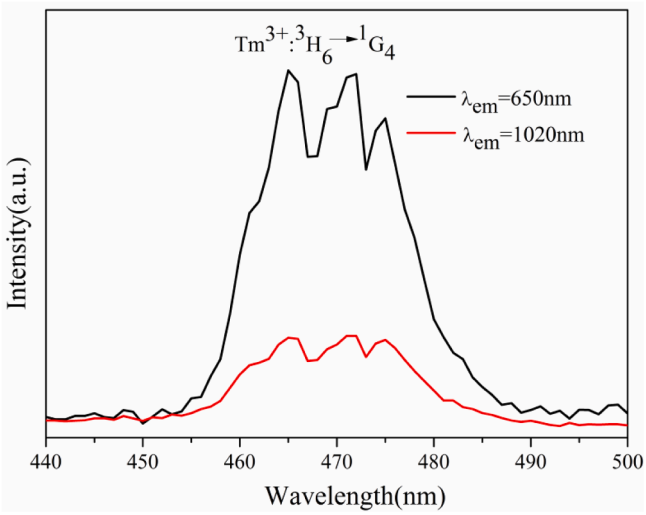

Fig. 6. Excitation spectra of TY9 sample monitoring at 650 and 1020 nm.

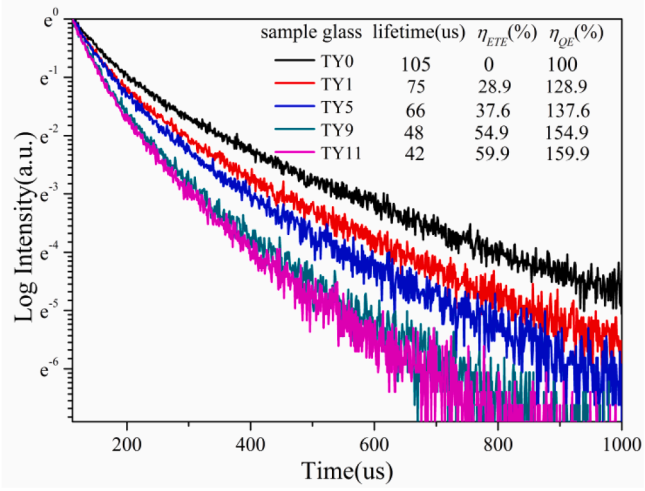

Fig. 7. Decay curves of Tm^{3+}:$^1G_4 \rightarrow {}^3F_4$ of TY samples excited by 467 nm.

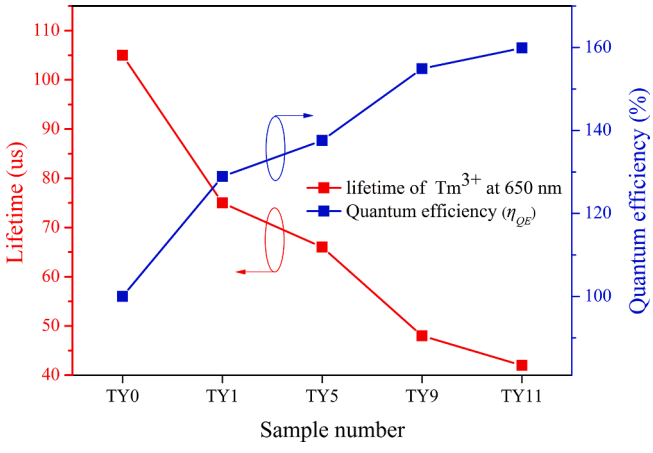

Fig. 8. Decay lifetime and quantum efficiency of TY samples.

Tm^{3+} to Yb^{3+} increases, thus intensity of Tm^{3+} $^1G_4 \rightarrow {}^3F_4$ emission decreases along with the life time at 650 nm decreases, This further proved the energy transfers between Tm^{3+} and Yb^{3+}.

Acorrding to the decay lifetime, the energy efficency (η_{ETE}) and the

quantum efficency (η_{QE}) can be caulated by the following equations [21–22,24]:

$$\eta_{ETE} = 1 - \frac{\tau_x}{\tau_0} \tag{3}$$

$$\eta_{QE} = \eta_{TM}(1 - \eta_{ETE}) + 2\eta_{ETE} \tag{4}$$

Here τ_x and τ_0 are the decay lifetimes of TY1-TY11 and TY0. The value of η_{TM} is set to 1 for neglecting the non-radiate energy loss by defects and impurities [21,25,26].

The concrete value of η_{QE} and η_{ETE} are demonstrated in Fig. 7, the trend of η_{QE} is shown in Fig. 8. The result illustrates the values of η_{QE} and η_{ETE} increase with the Yb^{3+} concentration increasement. As the concentrate of Yb^{3+} reach 11%, the η_{ETE} and η_{QE} come up to 59.9 and 159.9, it means that with increasement of the Yb^{3+} concentration, the cooperative energy transfer increases. So it is very meaningful use for the TY glasses used in silicon solar cells.

Conclusion

The quantum cutting between the Tm^{3+} and Yb^{3+} in phosphate glass was researched, the result shows existence of the cooperative energy transfer from Tm^{3+}: $^1G_4$ to Yb^{3+}: $^2F_{5/2}$. With the Yb^{3+} concentration increase, the energy transfer efficiency and Quantum efficiency increase, the maximum energy transfer efficiency and Quantum efficiency are up to 59.9% and 159.9%, the emission wavelength at 1020 nm is fitted the band gap of the crystalline Si, so these phosphate glasses can be used in silicon solar cells to improve the utilization of solar energy.

Declaration of Competing Interest

The authors declare that they have no known competing financial interests or personal relationships that could have appeared to influence the work reported in this paper.

Acknowledgment

This project was funded by the National Natural Science Foundation of China (No.51801001), school grade projects of Baoji University of Arts and Sciences (No. ZK15041).

References

[1] Tao J, Li B. Editorial : visible light-responsive photocatalysts for energy production. Front Chem 2019;7:304.
[2] Kannan N, Vakeesan D. Solar energy for future world: – a review. Renew Sust Energ Rev 2016;62:1092–105.
[3] Chang W, Li L, Dou M, Yan Y, Jiang S, Pan Y, et al. Dual-mode downconversion luminescence with broad near-ultraviolet and blue light excitation in Tm^{3+}/Yb^{3+} codoped oxy-fluoride glasses for c-Si solar cells. Mater Res Bull 2019;112:109–14.
[4] Richards BS. Enhancing the performance of silicon solar cells via the application of passive luminescence conversion layers. Sol Energ Mat Sol C 2006;90:2329–37.
[5] Zhou X, Shen J, Wang Y, Feng Z, Wang R, Li L, et al. An efficient dual-Mode solar spectral modification for c-Si solar cells in Tm^{3+}/Yb^{3+} codoped tellurite glasses. J Am Ceram Soc 2016;99:2300–5.
[6] Duan Q, Qin F, Wang D, Xu W, Cheng J, Zhang Z, et al. Quantum cutting mechanism in Tb^{3+}-Yb^{3+} co-doped oxyfluoride glass. J Appl Phys 2011;110:113503.
[7] Dexter DL. Possibility of luminescent quantum yields greater than unity. Phys Rev 1957;108:630–3.
[8] Lin H, Zhou S, Hou X, Li W, Li Y, Teng H, et al. Down-conversion from blue to near infrared in Tm^{3+}–Yb^{3+} codoped Y_2O_3 transparent ceramics. IEEE Photon Technol Lett 2010;22:866–8.
[9] Huang F, Chen L, Han Y, Tang J, Nie Q, Zhang P, et al. Visible to near-infrared down conversion in Tm^{3+}/Yb^{3+} co-doped chalcohalide glasses for solar spectra converter. Infrared Phys Techn 2015;71:159–62.
[10] Bouajaj A, Belmokhtar S, Britel MR, Armellini C, Boulard B, Belluomo F, et al. Tb^{3+}/Yb^{3+} codoped silica–hafnia glass and glass–ceramic waveguides to improve the efficiency of photovoltaic solar cells. Opt Mater 2016;52:62–8.
[11] Aarts L, Ende BVD, Reid MF, Meijerink A. Downconversion for solar cells in YF_3: Pr^{3+}, Yb^{3+}. Spectrosc Lett 2010;43:373–81.
[12] Duan Z, Zhang J, He D, Sun H, Hu L. Effect of CdF_2 addition on thermal stability and upconversion luminescence properties in Tm^{3+}–Yb^{3+} codoped oxyfluoride silicate glasses. Mater Chem Phys 2006;100:400–3.
[13] Pisarska J, Lisiecki R, Ryba-Romanowski W, Dominiak-Dzik G, Pisarski WA. Up-converted luminescence in Yb–Tm co-doped lead fluoroborate glasses. J Alloy Compd 2008;451:226–8.
[14] Yuan J, Wang WC, Chen DD, Peng MY, Zhang QY, Jiang Z H. Enhanced 1.8 μm emission in Yb3+/Tm3+ codoped tungsten tellurite glasses for a diode-pump 2.0 μm laser. J. Non. Cryst Solids, 402(2014), 223-230.
[15] Balaji S, Biswas K, Sontakke AD, Gupta G, Annapurna K. Enhanced 1.8 μm emission in Yb^{3+}/Tm^{3+} co-doped tellurite glass: effects of Yb^{3+}/Tm^{3+} energy transfer and back transfer. J Quant Spectrosc Ra 2014;147:112–20.
[16] Wang WC, Yuan J, Liu XY, Chen DD, Zhang QY, Jiang ZH. An efficient 1.8 μm emission in Tm^{3+} and Yb^{3+}/Tm^{3+} doped fluoride modified germanate glasses for a diode-pump mid-infrared laser. J Non Cryst Solids 2014;404:19–25.
[17] Wang WC, Yuan J, Liu XY, Chen DD, Zhang QY. Spectroscopic properties and energy transfer parameters of Yb^{3+}/Tm^{3+} co-doped fluorogermanate glasses. J Non Cryst Solids 2016;431:154–8.
[18] Zhang Q, Zhu B, Zhuang Y, Chen G, Liu X, Zhang G, et al. Quantum cutting in Tm^{3+}/Yb^{3+}-codoped lanthanum aluminum germanate glasses. J Am Ceram Soc 2010;93:654–7.
[19] Lakshminarayana G, Qiu J. Near-infrared quantum cutting in RE^{3+}/Yb^{3+} (RE= Pr, Tb, and Tm): GeO_2–B_2O_3–ZnO–LaF_3 glasses via downconversion. J Alloy Compd 2009;481:582–9.
[20] Dwaraka Viswanath CS, Babu P, Martin IR, Venkatramu V, Lavin V, Jayasankar CK. Near-infrared and upconversion luminescence of Tm^{3+} and Tm^{3+}/Yb^{3+}-doped oxyfluorosilicate glasses. J Non-Cryst Solids 2019;507:1–10.
[21] Lakshminarayana G, Yang H, Ye S, Liu Y, Qiu J. Co-operative downconversion luminescence in Tm^{3+}/Yb^{3+}: SiO_2–Al_2O_3–LiF–GdF_3 glasses. J Phys D Appl Phys 2008;41:175111.
[22] Li L, Pan Y, Chang W, Feng Z, Chen P, Li C, et al. Near-infrared downconversion luminescence of $SrMoO_4$: Tm^{3+}, Yb^{3+} phosphors. Mater Res Bull 2017;93:144–9.
[23] Guo Q, Liao L, Liu H, Mei L. Studies on Ce^{3+} positions and photoluminescence properties of $La_{1.45}Ce_{0.05}Ba_{3.5}(SiO_4)_{1.5}(PO_4)_{1.5}F$ phosphor. J Lumin 2016;178:1–5.
[24] Chen J, Liu Y, Fang M, Huang Z. Luminescence properties and energy transfer of Eu/Mn-coactivated $Mg_2Al_4Si_5O_{18}$ as a potential phosphor for white-light LEDs. Inorg Chem 2014;53:11396–403.
[25] Xu B, Yang B, Zhang Y, Xia H, Wang J. Cooperative energy transfer in Tm^{3+} and Yb^{3+} co-doped phosphate glasses. J Rare Earth 2013;31:164–8.
[26] Huang F, Chen L, Han Y, Tang J, Nie Q, Zhang P, et al. Visible to near-infrared downconversion in Tm^{3+}/Yb^{3+} co-doped chalcohalide glasses for solar spectra converter. Infrared Phys Techn 2015;71:159–62.